17th Australasian Fluid Mechanics Conference
Auckland, New Zealand
5-9 December 2010

Towards Large Eddy Simulation of Bubble Dispersion in High Reynolds Number Wake Flows

S. J. Zhu[1], H. M. Blackburn[2], B. Anderson[3] and A. Ooi[1]

[1]Department of Mechanical Engineering
The University of Melbourne, Victoria, 3010 AUSTRALIA

[2]Department of Mechanical and Aerospace Engineering
Monash University, Victoria, 3800 AUSTRALIA

[3]Maritime Platforms Division
Defence Science and Technology Organisation, Victoria, 3207 AUSTRALIA

Abstract

This study presents simulations of bubble dispersion in a free shear flow and cylinder wakes. The numerical method of a transient solver for two-dimensional incompressible flow with a subgrid-scale (SGS) turbulence model applied with the Lagrangian particle dynamics (LPD) method is proposed. The method is validated for the case of a free shear flow. The computed instantaneous bubble distribution and time averaged bubble concentrations agree well with both experimental and numerical data available in the open literature. The simulation of bubble dispersion over a cylinder is performed at Reynolds number of 9560. Bubble entrainment into the vortices in the cylinder wake is analysed. The results demonstrated the proposed method is able to reproduce the relevant physics of bubbly flows at high Reynolds numbers.

Introduction

Prediction of bubble distribution in ship wakes is an important naval research area. Bubbles trapped in the large vortical structures in the ship wake can form clusters that are able to persist for large distances, which increases the ship's detectability, an important consideration in the defence environment. Complete analysis of the problem requires complex modelling of the physics for both liquid and gas phases. With recent developments in computational capability, understanding the behaviour of bubbly flows by numerical simulation is becoming more common.

Two types of models are prevalent in the numerical simulation of dispersed bubbly flows, Eulerian-Lagrangian (particle tracking) and Eulerian-Eulerian (two-fluid) formulations. In the Eulerian-Lagrangian model, liquid is treated as a continuous phase that is solved using Navier-Stokes and continuity equations, and individual bubbles are tracked as dispersed phase. In the Eulerian-Eulerian model, each phase is treated as a continuous phase that is intermingled and interacting with the other phase based on the concept of volume or time averaging with different velocities and volume fractions. Both approaches have been used to model various flow applications, such as bubbly mixing layer [3], bubble columns ([8], [15]), and bubbly wake flows ([9], [12]). Considering relatively small amounts of bubbles (low void fractions) in the ship wakes, the method of Lagrangian particle tracking is most suitable for computing bubble distributions. It has advantages over the two-fluid method in the case of dilute suspensions or when large concentration variability of the discrete phase is present ([4], [5]). This situation is true for bubbly wake flows, such as those in ship wakes, where bubbles may experience preferential concentration and clustering effects in the near wake region but are rather dilute in the far wake [12]. Thus, the Eulerian-Lagrangian models are more suited for fundamental investigations of bubbly flow [10].

Simulations of bubbly turbulent flows require accurate representation of the fluctuating flow field that governs bubble dynamics. Direct numerical simulations (DNS) or large eddy simulations (LES) are often used to attain this accuracy [12]. DNS can provide detailed information of the flow field without the use of a turbulence model, but it is limited to low Reynolds number flows due to its high computational expenses. LES solves large scale turbulent eddy motions with a subgrid-scale (SGS) model that mimics the small scale motions. Thus, LES can handle high Reynolds number flows at a much reduced cost. A joint method of DNS combined with the Lagrangian particle dynamics (LPD) method was applied to simulate bubble dispersion over a cylinder and a hydrofoil at low Reynolds numbers in the previous work [16]. The simulations demonstrated that the interaction between the large scale eddies and the bubbles was successfully modelled and the bubble stream forms the characteristic "S" shape in the wake region that compares well with the corresponding experimental results [14]. However, no bubble entrainment into the vortex cores was observed in the numerical data as the vortices formed from the cylinder and the hydrofoil were not strong enough at low Reynolds numbers. In order to simulate bubbly flow at higher Reynolds numbers, a transient solver for two-dimensional incompressible flow with a SGS model is applied with the Lagrangian particle dynamics method. This is proposed as an intermediate step towards the LES of bubble dispersion in high Reynolds number wake flows.

In this paper, the proposed method is validated for the case of bubble dispersion in a free shear flow, which has been previously studied by Rightley and Lasheras [11] and Smirnov *et al.* [12]. It is confirmed that the simulated distributions of bubbles agree well with the measurements. Bubble entrainment in the flow over a cylinder at a high Reynolds number is also investigated.

Numerical Method for Incompressible Flow

Incompressible Navier-Stokes Equations

The analytical techniques applied in this numerical study are associated with time-integration of the incompressible Navier-Stokes and continuity equations

$$\frac{\partial u_i}{\partial t} + u_j \frac{\partial u_i}{\partial x_j} = -\frac{1}{\rho}\frac{\partial p}{\partial x_i} + \nu \frac{\partial^2 u_i}{\partial x_j x_j} \quad (1)$$

$$\frac{\partial u_i}{\partial x_i} = 0 \quad (2)$$

where u_i is the velocity components in the flow field, p, ρ and ν are respectively the fluid pressure, density and kinematic viscosity.

Subgrid scale model of eddy viscosity type

As DNS requires large amounts of gridpoints to resolved the flow field at high Reynolds numbers, it will be computationally cheaper to resolve the large scale of motions at the grid level and model the subgrid scale motions. Thus, equation (1) and (2) are spatially filtered with a grid filter (Δ). Mathematically, it is equivalent to break the velocity field into a resolved component (denoted by an overbar) and a subgrid component (denoted by a prime).

$$u_i = \overline{u}_i + u_i', \quad p = \overline{p} + p' \tag{3}$$

Substituting equations in (3) into equation (1) and (2) yields the filtered Navier-Stokes equations

$$\frac{\partial \overline{u}_i}{\partial t} + \overline{u}_j \frac{\partial \overline{u}_i}{\partial x_j} = -\frac{1}{\rho}\frac{\partial \overline{p}}{\partial x_i} + \nu \frac{\partial^2 \overline{u}_i}{\partial x_j x_j} - \frac{1}{\rho}\frac{\partial \tau_{ij}^S}{\partial x_j} \tag{4}$$

$$\frac{\partial \overline{u}_i}{\partial x_i} = 0 \tag{5}$$

where $\tau_{ij}^S = \overline{u_i u_j} - \overline{u}_i \overline{u}_j$ is the SGS stress tensor that arises from the non-linear advection terms and it represents the unresolved small scale structures

SGS models of the eddy viscosity type are based on the hypothesis that the deviatoric part of the SGS stress tensor is locally aligned with the filtered deviatoric part of the rate of strain tensor, while the normal stresses are assumed to be isotropic and are thus representable through a SGS kinetic energy [6]

$$\tau_{ij}^S = \frac{2}{3}kI + (\tau_{ij}^S)_D = \frac{2}{3}kI - 2\nu_T(\overline{S}_{ij})_D \tag{6}$$

where k is the SGS kinetic energy, I is the unit tensor, ν_T is the SGS viscosity, $(\tau_{ij}^S)_D$ is the deviatoric part of the SGS stress tensor and $(\overline{S}_{ij})_D$ is the deviatoric part of the rate of strain tensor, $\overline{S}_{ij} = \frac{1}{2}(\frac{\partial \overline{u}_i}{\partial x_j} + \frac{\partial \overline{u}_j}{\partial x_i})$.

k and ν_T can be derived from a $k^{-\frac{5}{3}}$ spectra assuming grid Reynolds number approaches infinity, and hence

$$k = c_I \Delta^2 |\overline{S}_{ij}|^2, \quad \nu_T = c_D \Delta^2 |\overline{S}_{ij}| \tag{7}$$

where the constants c_I and c_D can be solved with the dynamic model suggested by Germano *et al.* [7]. To keep the summary here brief, the reader is referred elsewhere [6] for a detailed description of the method.

Bubble Tracking Formulation

Bubbles in the flow experience the combined effects of the carrying fluid flow and the buoyancy force. Thus, a precise force balance acting on the bubbles is required. These forces include added mass, buoyancy, drag, lift and Bassett. The Bassett force term involves a time integral of the interactions of a bubble with its own wake and its contribution was concluded to be less than 6% of the buoyancy force [13]. As a consequence, this force is neglected in this study.

The bubble trajectories are obtained using the equations of motion from [8] and [13]

$$\frac{dU_b}{dt} = A_a + A_b + A_d + A_l \tag{8}$$

where U_b is the bubble velocity and A_a, A_b, A_d and A_l are the accelerations due to added mass, buoyancy, drag and lift.

Added mass: It is also known as virtual mass, which is the inertia added to a bubble as it is accelerating or decelerating in the fluid. The acceleration due to added mass is

$$A_a = C_a\left(\frac{\partial U_f}{\partial t} + (U_f \cdot \nabla)U_f\right) \tag{9}$$

where U_f is the fluid velocity and the coefficient of added mass (C_a) is found to be 3.0 assuming the bubble is spherical [13].

Buoyancy: The acceleration due to buoyancy is

$$A_b = -C_b g \tag{10}$$

where g is the gravity and the coefficient of buoyancy (C_b) is found to be 2.0 [13].

Drag: Acceleration due to drag is

$$A_d = -\frac{U_{rel}}{\tau_b} \tag{11}$$

where U_{rel} is the relative velocity between the bubble and fluid, τ_b is the relaxation time of the bubble responding to changes in the local flow velocity. In the case of bubbles with very small diameter (d_b), the bubbles respond as rigid spherical particles. Thus, particle relaxation time based on the bubble Reynolds number ($Re_b = |U_{rel}|d_b/\nu_f$) is

$$\tau_b = \begin{cases} \frac{\rho_b d_b^2}{18\rho_f \nu_f} & Re_b \leq 0.1 \\ \frac{4}{3}\frac{\rho_b d_b}{\rho_f C_d |U_{rel}|} & Re_b > 0.1 \end{cases} \tag{12}$$

where ν_f is the fluid kinematic viscosity, ρ_b and ρ_f are the density of bubble and fluid respectively. C_d is the coefficient of drag, which can be taken from the standard drag curve [2]

$$C_d = \begin{cases} \frac{24}{Re_b} & Re_b \leq 0.1 \\ \frac{24}{Re_b}(1 + 0.15 Re_b^{0.687}) & 0.1 < Re_b \leq 1000 \\ 0.44 & Re_b > 1000 \end{cases} \tag{13}$$

Lift: Acceleration due to lift is

$$A_l = -C_l(U_{rel} \times \omega) \tag{14}$$

where the coefficient of lift, C_l, was derived to be 0.53 [1] and ω is the vorticity.

Computational Details

A Free Shear Flow

The schematic of the computational domain for a free shear flow is shown in figure 1. The width of the domain is $l = 120$ mm and the inlet is divided into an upper (low speed) region and an lower (high speed) region. The outlet is located $3.6l$ downstream. Cells counts are 1080×360 in the streamwise and vertical directions. The high and low speed freestream velocities of 0.28 m/s and 0.07 m/s are applied at the lower and upper inlet boundary respectively. Columns of bubbles are injected into the high speed side of the free shear layer during the simulation.

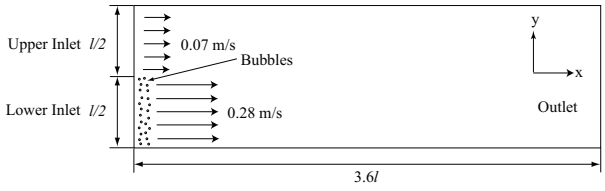

Figure 1: Free shear flow domain.

Flow over a cylinder

Figure 2 shows the computational domain of flow over a cylinder. The numerical parameters are chosen based on the experimental setup by [14]. The cylinder is modelled as a circle with a radius, $d = 27$ mm and a flow domain is created around it. The semi-circular inlet and flat outlet are located at $2.5d$ upstream and $6d$ downstream respectively. The width of the domain is $5d$. Cell counts are 150×810 in the radial direction (N_r) and wake direction (N_w). A freestream velocity u, which is based on the Reynolds number ($Re = ud/\nu$), is applied at the inlet, top and bottom boundaries.

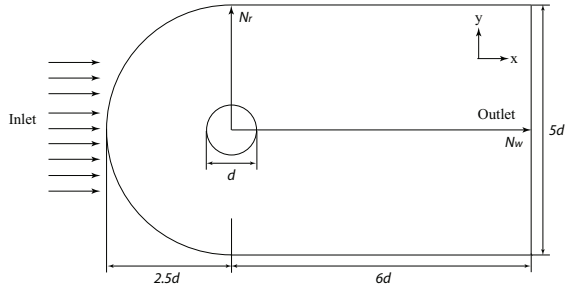

Figure 2: Flow over a cylinder domain.

Results

Validation on Bubble Dispersion in a Free Shear Flow

The validation of the joint transient solver with a turbulence SGS model and LGP method approach is performed for the case of bubble dispersion in a free shear flow. Rightley and Lasheras [11] investigated the interaction of a dilute dispersed cloud of microbubbles with a planar free shear layer experimentally. Smirnov *et al.* [12] performed the numerical study of the same flow with both the large eddy simulation (LES) and the LES with a random flow generation (RFG) technique.

In the simulation of bubble dispersion in a free shear flow, a column of 100 bubbles of 40 μm in diameter were injected from the high speed inlet with a time interval of 25 ms for a duration of 15 s. Figure 3 shows a comparison of instantaneous visualisation of bubble distribution from experiment [11] and computed data. Both figures are captured at different time instance, but

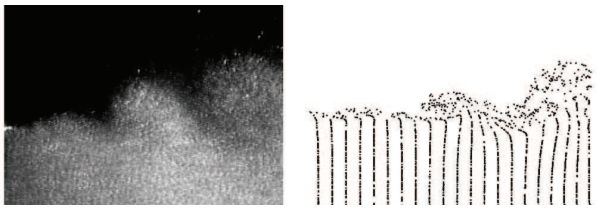

Figure 3: Instantaneous visualisation of bubble distribution: left: experimental bubble distribution [11], right: computed bubble distribution.

similar bubble dynamic features are well shown in both of the figures. Bubbles can be seen enter into the low speed layer from the high speed layer due to the entrainment into the coherent vortex structures in the mixing region.

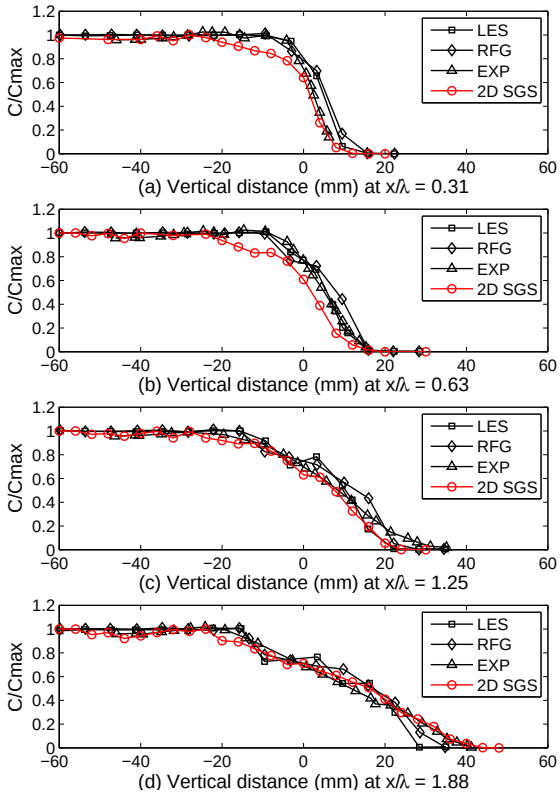

Figure 4: Comparison of normalised mean bubble concentrations: □ - LES [12], ◊ - LES/RFG [12], △ - experiment [11] and ◯ - 2D transient solver with a SGS model.

Comparisons of the time averaged bubble concentration against both the experimental and numerical data at different downstream locations of the free shear flow are shown in figure 4. The local bubble concentration (C) is normalised with the maximum bubble concentration (Cmax) in the flow field. It can be seen that the data from current method agrees reasonably well with [11] and [12] except that the bubble concentrations in the region between -20 mm to 0 mm vertically at the locations of $x/\lambda = 0.31$ and 0.63 (where λ is the billow-to-billow distance ≈ 0.8 m) are slightly underpredicted.

Bubble Dispersion over a Cylinder

Experimental work of bubble behaviour in the wake of a circular cylinder was conducted by [14]. In the experiments, the flow is generated by a water pump and the water flow rate can be adjusted by a pump controller to achieve different Reynolds

numbers. Air bubbles of 2 mm in diameter are injected through a nozzle at the bottom of the water tunnel with a cylinder of 27 mm in diamter mounted on the cylinder holder.

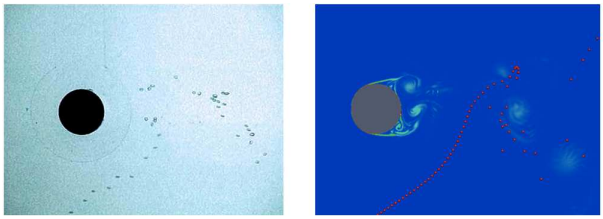

Figure 5: Bubble dispersion in the cylinder wake at Re = 9560: left: experimental bubble distribution, right: computed bubble distribution with the vorticity magnitude contour.

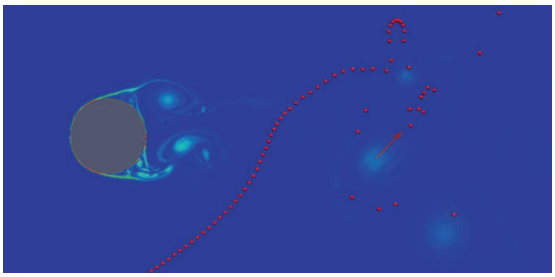

Figure 6: Bubbles escape from the weakened vortices with the vorticity magnitude contour.

The numerical investigation on the bubble behaviour in the cylinder wake at Reynolds number of 9560 is performed. The simulation setup corresponds to the experiment by Tho and Vassallo [14]. Both experimental and numerical results of bubble distribution in the cylinder wake are shown in figure 5. From the experimental results, the bubble stream enters into the wake region forming the characteristic "S" shape and bubbles are then pushed downwards into the wake region while they turn in the direction of the freestream near the upper boundary of the wake, which forms distinct bubble packets behind the cylinder. Similar results are observed in the numerical data. It can be seen that two bubble packets are formed when bubbles are entrained into the two vortices developed from the cylinder. As shown in figure 6, bubbles are found to escape from the vortices while they are propagating downstream as the strength of the vortices weakens.

Conclusions

Numerical simulations of bubble dispersions for a free shear flow and cylinder wakes are obtained using the approach of a transient solver with a SGS turbulence model and the LPG method. The motivation for this study is that the approach of DNS with LPG method is limited to low Reynolds number flows due to the high computational expenses.

As a validation case, simulation of bubble dispersion in a free shear flow is performed. The evolution of the bubble cloud is evidently dominated by the influence of the large scale coherent structure developed in the mixing region. The spatial development of normalised averaged bubble concentration agrees well with both experimental and numerical data. Simulation of bubble dispersion over a cylinder at Reynolds number of 9560 is also performed. The characteristic "S" shape formed by a bubble stream in the cylinder wake is captured in the numerical data. It is further found that the bubble escape mechanism is due to the combined effects of the weakening of vortex strength and buoyancy force.

The results of this study show that the approach of a transient solver with a SGS turbulence model with the LPG method can be successfully implemented in the high Reynolds number bubbly flows and the method is able to accurately reproduce the relevant physics of bubble dispersion.

References

[1] Auton, T. R., The dynamics of bubbles, drops and particles in motion in liquids, Ph.D. Thesis, Cambridge University, Cambridge, UK, 1981.

[2] Clift, R., Grace, J. R. and Weber, M. E., Bubbles, drops and particles, Academic Press, New York.

[3] Climent, E., and Magnaudet, J., Dynamics of a two-dimensional upflowing mixing layer seeded with bubbles: Bubble dispersion and effect of two-way coupling, *Phys. Fluids*, **18** (10), 2006, 103304.

[4] Crowe, C. T., An assessment of multiphase flow models for industrial applications, in *Proc. FEDSM'98*, volume FEDSM-5093, Washington, DC, USA, 1998.

[5] Elghobashi, S., On predicting particle-laden turbulent flows, *Appl. Sci. Res.*, **52**, 1994, 309–329.

[6] Fureby, C., Tabor, G., Weller, H. G., and Gosman, A. D., A comparative study of subgrid scale models in homogeneous isotropic turbulence, *Phys. Fluids*, **9** (5), 1997, 1416-1429.

[7] Germano, M., Piomelli, U., Moin, P., and Cabot, W. H., A dynamic subgrid-scale eddy viscosity model, *Phys. Fluids A*, **3** (7), 1991, 1760-1765.

[8] Hu, G. and Celik, I., Eulerian-Lagrangian based large-eddy simulation of a partially aerated flat bubble column, *Chem. Eng. Sci.*, **63**, 2008, 253-271.

[9] Nishikawa, H., Matsumoto, Y. and Ohashi, H., Numerical calculation of the bubbly two-phase flow around an airfoil, *Comput. Fluids*, **19**, 1991, 453460.

[10] Pan, Y., Dudukovic, M.P., and Chang, M., Dynamic simulation of bubbly flow in bubble columns, *Chem. Eng. Sci.*, **54(13)**, 1999, pp.2481-2489.

[11] Rightley, P. M., and Lasheras, J. C., Bubble dispersion and interphase coupling in a free-shear flow, *J. Fluid Mech.*, **412**, 2000, 21-59.

[12] Smirnov, A., Celik, I., and Shi, S., LES of bubble dynamics in wake flows, *Comput. Fluids*, **34**, 2005, 351–373.

[13] Sridhar, G., and Katz, J., Drag and lift forces on microscopic bubbles entrained by a vortex, *Phys. Fluids*, **7** (2), 1995, 389-399

[14] Tho, P., and Vassallo, S., Bubble behaviour in the wake of circular cylinders, Final Year Research Project, The University of Melbourne, Melbourne, Australia, 2002.

[15] Viviek, V., Dhanannjay, S. D. and Viviek, V. R., Eulerian-Lagrangian simulations of unsteady gas-liquid flows in bubble columns, *Int. J. Multiphase Flow*, **32**, 2006, 864-885.

[16] Zhu, S. J., Ooi, A., Blackburn, H. M., and Anderson, B., Validation of numerical model for bubble dispersion over a hydrofoil, in *Proc. IEEE Oceans 2010*, Sydney, Australia, 2010.